Mon. Not. R. Astron. Soc. **000**, 1–9 (2002) Printed 18 June 2013 (MN LATEX style file v2.2)

How abundant are the Local Group galaxies?

fulano, perano mengano. Disc survival collaboration UdeA-AIP[12]
[1] *Leibniz-Institut Für Astrophysik Potsdam, An der Sternwarte 16, 14482 Potsdam, Germany.*
[2] *Instituto de Fisica, Universidad de Antioquia, Medellin, Colombia.*

Accepted XXXX December XX. Received XXXX December XX; in original form 2009 June 27

ABSTRACT

We present a series of models that follow the evolution of the two dominant galaxies in the Local Group: the Milky Way (MW) and M31. We use semi-analytic techniques coupled to three N-body constrained cosmological simulations. Each simulated volume contains a pair of halos with environmental conditions similar to the observed for the LG. The models are computed using the public available code Galacticus. The main objective is to study the conditions to get the best possible agreement in three baryonic properties for the MW and M31: the stellar mass, gaseous mass and disc-to-bulge mass ratio. Each physical model varies the parameters controlling the star formation efficiency and supernovae feedback. The models are run on a general sample of dark halos with a mass range of $7 \times 10^{11} h^{-1}\,\mathrm{M}_{\odot} < \mathrm{M_h} < 7 \times 10^{12} \mathrm{h}^{-1}\,\mathrm{M}_{\odot}$. For the model that best reproduce the global properties of galaxies in this halo mass range, we find that the most probable values for the baryonic properties are $M_{\star} =$, $M_{\mathrm{gas}} =$ and $f_{D/B} =$. The three LG in the constrained simulation have values $M_{\star} =$, $M_{\mathrm{gas}} =$ and $f_{D/B} =$.

Key words: galaxies: haloes, groups – cosmology: dark matter, observations

1 INTRODUCTION

cosmological scenario the local group the problem of locating the LG in the universe

The questions we want to address in this paper is: How common is the local group of galaxies in the cosmological context? what is the probability of generate a local group in the universe? under which physical conditions do we reproduce the properties of the galaxies in the Local Group?

2 METHODS

2.1 N-body simulations

In this work we study the evolution of galaxies in the Local Universe through the use of semi-analytic models of galaxy formation. To properly constrain the study to the Local Group it is required to use then constrained simulations of the Local Universe. A constrained simulation is a standard N-body simulation of the formation of structure in which observational constraints have been imposed on the initial conditions in order to reproduce the large scale environment of the local Universe. The simulations used in this work have been extensively discussed in previous works, we refer the reader seeking for a detailed description of the procedures and details of the simulations to these papers (Martinez-Vaquero et al. 2009, Gottlöber et al. 2010, Forero-Romero et al. 2011, Doumler et al. 2012). Here we will focus only on the details of the simulations that are relevant for the sake of interest of this paper.

The constrained simulations used in this work are part of a suite of cosmological simulations part of the CLUES project (Constrained Simulations of the Local Universe, Gottlöber et al. 2010). The observational constraints impose conditions on the large scale structure of the local Universe on scales above a few mega parsec, however the small scales keep unconstrained and behave basically randomly. In order to overcome this problem, and to obtain a realisation that matches as close as possible not only the large scale environment but also the environment of the Local Group, many realisations are required of the same piece of the Universe with the same constraints. From this set of realisations a few have been selected to be potential candidates in which not only the large scale environment but also the small scale environment have been satisfactorily reproduced.

The criteria used to identify fiducial a Local Group realisation among this set of 200 are (see Forero-Romero et al. 2011)

- The distance between neighbour haloes is smaller than $0.7h^{-1}$ Mpc (Ribas et al. 2005)
- The relative radial velocity of the two haloes is negative.
- There must be no objects more massive than either of

© 2002 RAS

the LG host haloes within a radius of $2h^{-1}$ Mpc from each other (Tikhonov & Klypin 2009)

- There must be no a halo of mass $> 5.0 \times 10^{13} h^{-1}\,\mathrm{M}_{\odot}$ within a radius of $5h^{-1}$ Mpc with respect to each halo centre (Karachentsev et al. 2004)

From a set of 200 low resolution realisations, only three were found to meet the aforementioned conditions to host a potential local group. These three simulations where resimulated at higher resolution with a box size of 64 h^{-1} Mpc and sampled with 1024^3 particles giving a particle mass of $1.89 \times 10^7\ h^{-1}\,\mathrm{M}_{\odot}$. The candidates to Milky Way (MW) and Andromeda galaxy (M31) in these simulations are resolved with more than 50000 particles. Simulations were performed with the cosmological Tree-PM code Gadget-2 (Springel 2005) and the starting redshift of the simulations was 50.

The use of the constrained simulations provide us with the unique opportunity to model the large and small scale environment of the Local Group, and pick candidate objects to host the M31 and M31 galaxies. Simultaneously, the realisation of simulations of dark matter only provide us with the opportunity to simulate a large sample of galaxies. For each of the three simulations we have around 10000 haloes identified with more than 200 particles, and around 9000 haloes in the mass range $10^{11} M_{\odot}$ to $10^{13} M_{\odot}$. In general, combining the three data sets we have a total of 27000 haloes in the mass range of $10^{11} M_{\odot}$ to $10^{13} M_{\odot}$, which provide us with a large statistical sample of MW type haloes.

In our simulations halos are identified using a FoF method with a linking lenght of $b = 0.17$ times the mean interpartilce distance and a at least 20 member particles. Haloes are identified in 80 snapshots roughly equally spaced in time between $z = 0$ and $z = 7$. The merger tree construction is based on the comparison of the particles in FOF groups in two consecutive snapshots. Starting at $z = 0$ for every FOF group in the catalog, G0, we find all the FOF groups in the previous snapshots that share at least thirteen particles with G0 and label them as tentative progenitors. Then, for each tentative progenitor, we find all the descendants sharing at least thirteen particles. Since the smallest FOF groups contain 20 particles at least 2/3 of the particles must be identified in tentative progenitors or descendants. Only the tentative progenitors that have as a main descendant the group G0 are labeled as confirmed progenitors at that level. We iterate this procedure for each confirmed progenitor, until the last available snapshot at high redshift. By construction, each halo in the tree can have only one descendant, but many progenitors

The merger histories used in this work have been studied in detail in Forero-Romero et al. 2011, we recommend the reader to take a look on this paper to find more details on the tree construction and the properties of the merger histories we use in this work.

2.2 Semi-analytic Modelling

Since the simulations we use are dark matter only, galaxy formation has to be modelled as an external process happening inside dark matter haloes. One of the advantages of using this semi-analytic approach is the opportunity to explore the parameter space and to find the parameter set that best reproduce the observed structure of the Local Group galaxies.

Instead of developing our own semi-analytic code of galaxy formation, we opted for the alternative to use a publicly available one. The code we used in this work is GALACTICUS, a semi-analytic code developed by Andrew Benson (Benson 2012). GALACTICUS implements several physical processes and implements different approaches for each process. Instead of exploring the many different possibilities of the code, we keep close to the "default model" of the code and used standard recipes to model the different physical processes as described in (Benson 2012).

In our simulations we have included many different physical processes: Radiative cooling, star formation, energy feedback processes, chemical enrichment, mass transfer between components, galaxy mergers, galactic structure, etc. No AGN feedback has been considered since we focus on a low halo mass regime where AGN effect should not play an important role.

Each physical process is controlled by one or more parameters. From that large set of physical processes we focus our attention on a few ones, under the assumption that these processes are the ones that most affect the final state of the galaxies forming inside the haloes of the simulation. For these models we have decided to vary systematically its parameters in order to explore the parameter space associated with the probability of having Local Group like galaxies (LG-like galaxies). After exploring the parameter space, we choose to study in detail the changes in the population of galaxies under variations of the physical parameters controlling the star formation time scale ($\epsilon_\star$, $\alpha_\star$), supernovae feedback ($\alpha_{\rm out}$) and the mass ratio defining the major/minor merger threshold.

2.2.1 Galaxy mass growth

One would expect that the accretion of cold gas in a dark matter halo depends on the mass growth rate of the halo, but also on the available gas mass, the mass of the halo itself and the thermodynamical conditions of the gas. In GALACTICUS we use the *simple* method to model the accretion of cold gas like

$$\dot{M}_{\rm accr} = \begin{cases} (\Omega_b/\Omega_M)\dot{M}_{\rm halo} & \text{if } V_{\rm vir} > V_{\rm reioniz} \\ & \text{or } z > z_{\rm reioniz} \\ 0 & \text{otherwise} \end{cases} \quad (1)$$

where Ω_b/Ω_M is the cosmic baryon fraction that basically controls the amount of available baryons and $V_{\rm reioniz}$ and $z_{\rm reioniz}$ are the free parameters that control the accretion of cold gas accretion. If a halo has a low virial velocity $V_{\rm vir}$ (lower than the threshold $V_{\rm reioniz}$) it is not massive enough to accrete and keep the cold gas. Also, if the redshift is larger than $z_{\rm reioniz}$ the temperature of the gas should be high enough and no effective cooling should be present.

2.2.2 Star formation time scale

We have used the standard Cole et al. 2000 star formation time scale. It is parametrised by a power law in the halo velocity

$$\tau_\star = \epsilon_\star^{-1} \tau_{\rm dyn} \left(\frac{V}{200{\rm km/s}} \right)^{\alpha_\star} \quad (2)$$

with free parameters $\epsilon_\star$ and $\alpha_\star$ that controls the star formation efficiency and the shape on the velocity (or mass) dependence of the star formation time scale.

2.2.3 Supernova feedback

The main energy feedback process of the model is the supernova feedback. Mass ejection from supernovae is modeled as

$$\dot{M}_{\rm out} = \left(\frac{V_{\rm out}}{V} \right)^{\alpha_{\rm out}} \frac{\dot{E}}{E_{\rm canonical}}, \quad (3)$$

where $V_{\rm out}$ is a threshold velocity for the galactic component. The larger the value of $V_{\rm out}$ the stronger the suppression of the outflow of mass. The second parameter is $\alpha_{\rm out}$, and as $\alpha_\star$ controls the mass dependence of the outflow. V, $\dot{E}$ and $E_{\rm canonical}$ are not constants, they are the velocity of the component, the rate of energy input from the stellar populations and the energy input by a stellar population normalised to $1{\rm M}_\odot$ after an infinite time.

2.2.4 Minor/Mayor merger (η)

We define a minor merger between a massive halo M_{Hm} and a low mass halo M_{Lm} if

$$\frac{M_{Lm}}{M_{Hm}} \leqslant \eta \quad (4)$$

where η is the threshold that defines the nature of the merger. In other case the merger will represent a major merger.

2.2.5 Merger mass flow

After a minor or major merger the mass of the galaxies must be redistributed in the remnant. The way the mass is redistributed in the remnant depends on the characteristics of the merger.

- If the merger is a major merger the structure of both galaxies is destroyed and all mass from both galaxies moves to the spheroid of the remnant central galaxy.
- In the case of a minor merger the mass of the satellite moves to the component that is indicated by the respective flag *goes to*, $M_{\rm satel.,gas} \rightarrow$, where in our case gas and stars can move from the satellite to the disk or to the bulge of the central galaxy.

2.2.6 Galaxy structure: Spin and concentration parameter

The structural properties of the galaxy depend partially on the structural properties of the dark matter halo. We used the approach included in GALACTICUS that allows to use the fitting formulae of Prada et al. 2011 to model the concentration parameter of halos as a function of mass and redshift. For the spin parameter we assume that this parameter follows a log-normal distribution with mean $\mu_\lambda = 0.031$ and variance $\sigma_\lambda = 0.57$ as computed from cosmological simulations by Muñoz-Cuartas et al. (2011).

Property	MW	Ref.	M31	Ref.
$M_{d,\star}[10^{10} M_\odot]$	$3.3 - 4.5$	(1)	$7 - 10$	(2)
$M_{d,gas}[10^{10} M_\odot]$	$0.6 - 0.8$	(3)	$0.5 - 0.6$	(4)
$M_{b,\star}[10^{10} M_\odot]$	$0.5 - 1.2$	(3)	$1.9 - 3.3$	(2)
$V_{\rm cmax}$[Km/s]	238	(5)	275 ± 5	(6)

Table 1. Observational estimations for different properties of the LG, where(1)**?**,(2) **?**, (3)**?**, (4) **?**, (5)**?**, (6)**?**.

2.3 Observational samples and definition of our local group

We have already shown in section 2.1 how do we define the Local Group galaxy candidates in our simulations. Now we need to introduce an operational definition for these galaxies from the observational point of view in order to be able to compare the observations with our simulations. Clearly, MW and M31 are characterised by its observational properties. Considering the quantities we can reliably model using the semi-analytic approach we define or characterise the LG galaxies according to the observed values of their disk stellar mass ($M_{d,\star}$), disk mass gas $M_{d,gas}$, bulge stellar mass $M_{b,\star}$ and maximum circular velocity $V_{\rm cmax}$.

Disk stellar mass. The principal approach to estimate the stellar mass in the disk of our galaxy is dynamical modelling. The work of **?** uses a parametric model that does not distinguish between the cold (gas) component and the stars, their results for galaxy models that allow for exchange of angular momentum locate the total baryonic mass of the disk between $5 - 6 \times 10^{10} M_\odot$ for the MW and $7 - 9 \times 10 M_\odot$ for M31. Later **?** use N-body realisations of self-consistent equilibrium distributions of the dark matter and stellar components to address the same problem. Their models with good match to the observational data have stellar masses of $3.3 - 4.5 \times 10^{10} M_\odot$ for the Milky Way and $7 - 10 \times 10^{10}$ for Andromeda. (**?**) modeled the Andromeda stream using analytic bulge-disc-halo models for M31, finding the best agreement for a disk mass of $8.4 \times 10^{10} M_\odot$. In this work we take $3.3 - 4.5 \times 10^{10} M_\odot$ for the Milky Way and $7 - 10 \times 10^{10}$ for M31.

Bulge stellar mass. **?** constrain the MW bulge stellar mass to $1 - 1.2 \times 10^{10}$ $M_\odot$ while for M31 $1.9 - 2.4 \times 10^{10}$. For the same galaxy (**?**) find a bulge mass of $3.3 \times 10^{10} M_\odot$. The MW analytic model of (**?**) finds a range of different values with average $\sim 0.5 10^{10} M_\odot$. In this work we pick $0.5 - 1.2 \times 10^{10} M_\odot$ for the MW and $1.9 - 3.3 \times 10^{10} M_\odot$ for M31.

Disk Gaseous mass. The abundance of gas in the Milky Way has been constrained through chemical evolution models. The set of observational constraints on these models most notably include the gas and star formation rate (SFR) profiles. The relevant observational data was compiled in (**?**) based on the original work in **??**, with values of $6.0 - 8.0 \times 10^9 M_\odot$. An updated implementation of this chemical evolution model by (**?**) uses the same observations. In the case of M31 the best observational constraints come from

the observations by (**?**) with the integrated mass of neutral gas corrected by (**?**), yielding a value of $5.2 \times 10^9 M_\odot$, there is a systematic observational uncertainty of 5% originally quoted in (**?**), but due to opacity effects of the HI (**?**) the total value of gas can increase by a 19%. Therefore we keep a value of $5.0 - 6.0 \times 10^9$ for the mass of gas in the M31 disk and $6.0 - 8.0 \times 10^9 M_\odot$ for the Milky Way.

Table 1 summarises the values we used to define each LG-like galaxy, including error bars, which will be important for the comparison analysis.

2.4 Analysis strategy

In this work we have two goals. First to determine quantitatively which is the probability to find a galaxy like MW and M31 in a given cosmological volume. Second, we want to see which are the values of the parameters in the model that maximise the probability of finding such galaxies.

To do so we have already defined quantitatively how a LG-like galaxy should look like, but we need to quantify how far are our models from such a definition. From this distance measure we can quantify the probability of finding LG-like galaxies in the nearby universe.

We define the distance between two galaxies (the defined MW or M31 and a model galaxy, where by model galaxy we mean one of our 27000 galaxies in our simulations) through the distance measure d defined as

$$d = \sqrt{\sum_{i=1}^{N} \left(\frac{y_i - m_i}{m_i} \right)^2} \qquad (5)$$

The distance d indicates the actual distance measure (or difference) between two points in a space defined by the parameter set m_i. The parameter set m_i is the set of values of quantities associated with the definition of our LG galaxies, that is, N=4 and m_i refers to $M_{d,*}$, $V_{\rm cmax}$, $M_{d,gas}$ and $M_{b,*}$ as they appear in table 1. The numbers y_i are the values associated with those quantities for each model galaxy in our simulations.

We then compute the value of the distance d from each model galaxy to the defined galaxies MW and M31 and trough it we quantify the probability to find such an object in our simulations.

3 RESULTS

Now we present the results of our research. First in section 3.1 we analyse, without considering the constrained nature of our simulations, which is the fraction of galaxies similar to our LG galaxies. To do that we use around 27000 central galaxies hosted in the same number of dark matter haloes in the mass range $10^{11} h^{-1}\,{\rm M}_\odot$to$10^{13} {\rm h}^{-1}\,{\rm M}_\odot$ and use the distance measure 5 to quantify the proximity of the models to the observations.

Later in section **??** we use explicitly the candidates to MW and M31 from our three realisations and study how variations on the parameters (α, ϵ) affect their properties, and specifically, how do these variations produce model galaxies that are in agreement with the observational constraints.

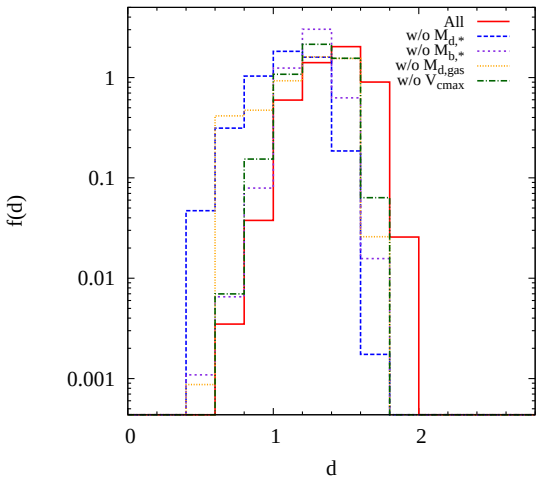

Figure 1. Distribution of d values for the same run (R1) computed using four different definitions of the distance measure as described in the text.

3.1 On the fraction of Local Group galaxies

First we check that our procedure defines robustly the distance measure to a LG-like galaxy. One may think that including or removing one of the quantities m_i from the definition of distance measure eq. 5 the distribution of values of d could change so much that the definition of distance is not robust enough, affecting drastically our probability estimates and conclusions. To verify the robustness of the distance measure we compute d removing cyclically one of the properties used to define it, i.e., using only $M_{d,*}$, $M_{d,gas}$ and $M_{b,*}$ or using only $M_{d,gas}$, $M_{b,*}$ and $V_{\rm cmax}$, and so on. Using this check we can see which is the impact of the specific physical quantity on the distance measure. Clearly, if variations on the definition leads to catastrophically different distributions of d, it will means that the defined distance measure is not robust enough and therefore is not an appropriated measure to quantify the probability of finding LG-like galaxies.

Figure 1 shows the distribution of distances d computed for the same run (R3 in table 2). The distance measure is computed for the MW galaxy using all the four galaxy properties, and respectively without the use of the $M_{d,*}$, $M_{b,*}$, $M_{d,gas}$ and without the use of $V_{\rm cmax}$ for the determination of the distance d.

Note that although in all cases the mode of the distribution places around the same position $d = 1.2$, the shape of the distribution is almost the same in all cases as well as its width. Note also that if well the change in the definition does affect the probability distribution, for example increasing the fraction of galaxies closer to WM type for definitions in which $M_{d,*}$ is not considered in to the definition, the differences keep small.

Note that in general no mass constraint is being used (remember that we ran this analysis on a population of haloes in the mass range from 10^{11} to $10^{13} M_\odot$), so, in principle the scatter we have is naturally due to the broad halo mass range we are exploring. Reducing the size of halo mass range clearly would lead to a smaller scatter, but in no way

Model	$z_{reioniz}$	$M_{\rm satel.,gas} \rightarrow$	η	$P(\lambda)$	μ_λ	σ_λ	$\alpha_{\rm disk,outflow}$	$\epsilon_{\rm disk,\star}$
R2	7.0	bulge	0.3	Lognormal	0.031	0.57	2.0	0.01
R3	7.0	disk	0.3	Lognormal	0.031	0.57	2.0	0.01
E1	7.0	disk	0.3	Lognormal	0.031	0.57	2.0	0.02
E2	7.0	disk	0.3	Lognormal	0.031	0.57	2.0	0.035
E3	7.0	disk	0.3	Lognormal	0.031	0.57	2.0	0.05
E4	7.0	disk	0.3	Lognormal	0.031	0.57	2.0	0.075
E5	7.0	disk	0.3	Lognormal	0.031	0.57	2.0	0.1
A1	7.0	disk	0.3	Lognormal	0.031	0.57	1.5	0.01
A2	7.0	disk	0.3	Lognormal	0.031	0.57	2.5	0.01
A3	7.0	disk	0.3	Lognormal	0.031	0.57	3.0	0.01
D1	7.0	disk	0.2	Lognormal	0.031	0.57	2.0	0.01
D2	7.0	disk	0.4	Lognormal	0.031	0.57	2.0	0.01
B1	7.0	bulge	0.2	Lognormal	0.031	0.57	2.0	0.01
B2	7.0	bulge	0.4	Lognormal	0.031	0.57	2.0	0.01

Table 2. Set of four experiments intended to model the galaxies hosted in halos of mass range of $11.0 < \log_{10} M_{\rm DM} < 13.0$.

it would lead to an increase in the frequency at the low d tail of the distribution.

We conclude that in general our definition of distance measure is robust enough to make an initial estimate on the distribution of galaxies in comparison with the LG-like galaxies and that our conclusions are robust enough.

Once we see that our distance measure is robust enough and that it is not biased by our choice of physical quantities, we can move to the analysis of the distribution of the distance measure for the LG-like galaxies. In Figure 2 we show the probability distribution of the distance measure for the set of runs associated to variations of the parameter $\alpha_{\rm out}$ for both, MW and M31 galaxy. As it can be seen in the figure, and in agreement with the previous experiment, for a given galaxy no major variations on the distribution of the distance measure are observed. The peak places closer to the same position shown in the previous experiment but the distribution clearly shows a tail to low d values, which is more extended for M31 than for MW. In general this means that the probability of finding objects like M31 is larger than that of finding MW-like objects. Note also that in general there is not a very strong variation on $f(d)$ for the different values of $\alpha_{\rm out}$. Only a mild increase in the probability of finding the galaxies with small d values at expenses of the respective decrement for the distribution at larger d values when $\alpha_{\rm out}$ increases from 1.5 to 3.0. This change is more evident for M31 where we can see that the frequency of d values (and therefore the probability) increases from ~ 0.0002 for $\alpha_{\rm out} = 0.15$ to ~ 0.001 for $\alpha_{\rm out} = 0.3$. A similar trend may be seen in the case of MW but since its distribution is more concentrated is not as noticeable as in the case of M31. This behaviour might imply that indeed higher values of $\alpha_{\rm out}$ may be needed if one requires to produce a large sample of LG-like galaxies, or equivalently, that LG-galaxies may be better characterised by high values of $\alpha_{\rm out}$.

A similar behaviour can be seen in Figure 3 where we show the distribution of d for MW and M31 for the experiment where the parameter under variation is $\epsilon_{\rm D,\star}$. For the different values of $\epsilon_{\rm D,\star}$ the distribution shows to be more skewed to low d-values than the distribution of the respective experiment for $\alpha_{\rm out}$, indicating that changes on $\epsilon_{\rm D,\star}$ may influence strongly the probability of finding galaxies like those in the Local Group. Nevertheless the differences in the distribution for different values of $\epsilon_{\rm D,\star}$ are not so big, and in particular low values of $\epsilon_{\rm D,\star}$ may favour the increased fraction of galaxies similar to these in our defined Local Group.

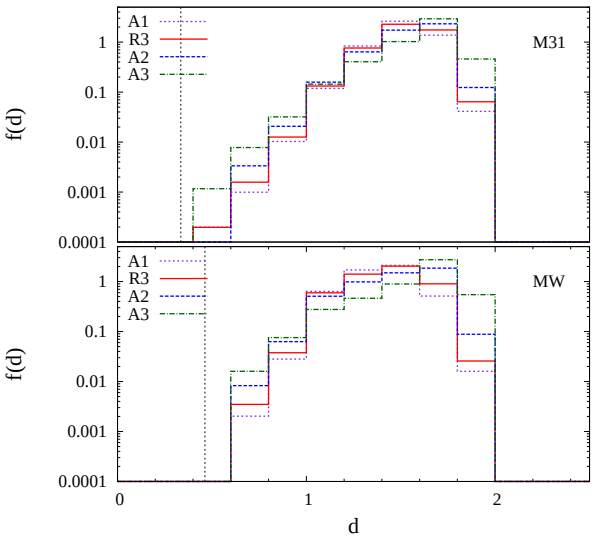

Figure 2. Distribution of d values relative the MW and M31 galaxies. The different lines correspond to realisations of the galaxy catalogue using models in which variations of $\alpha_{\rm out}$ where carried out from 0.15 to 0.3 while keeping constant the other model parameters. See table 2 for more information about the model parameters.

In these figures the vertical lines correspond to the maximum d value supported by the observations. It is computed using eq. 5 but instead of using in y_i the values of any model galaxy, we used the values of $m_i + \Delta m_i$, that is, just the square root of the sum of the squares of the relative errors of the measurements. Under the definition of the distance d

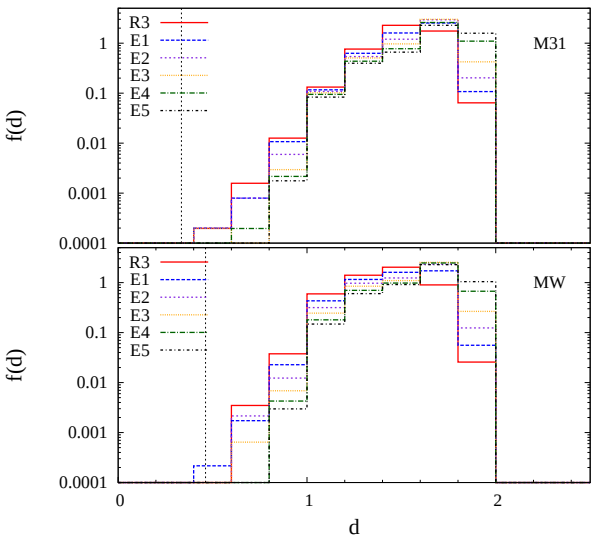

Figure 3. The same as in figure 2 but this time with variations on $\epsilon_{D,\star}$ from 0.01 to 0.1. See table 2 for more information about the model parameters.

this should be the maximum distance at which the observations are in agreement with themselves, and then, indicates the region below which any model fits the observations. As it can be seen in the figures, no model fits the definition to be a MW or M31 galaxy, i.e. the fraction of LG-like galaxies in our simulations, according to our definition and our distance measure, is zero.

We conclude two things from this comparison. First, if well the values of the model parameters modify the population of galaxies, relative to LG-like ones, the changes are not so dramatic in the sense that the number of LG-like galaxies does not change. Second, under the distance measure used in this work, it results too difficult to fit simultaneously all observables of LG-like galaxies, even if the environment has been set up to reproduce that of the LG.

These results clearly posses a problem: How is it possible to have a sample of 27000 galaxies, some of them being hosted in dark matter haloes that are dynamically and environmentally selected to be good candidates to host LG-like galaxies but finally none of these galaxies fits our definition of LG-like galaxy?

Relaxing the definition of LG galaxies leads to what we see in figure 4 [1] where we have used only one quantity to define the distance measure between our models and the LG galaxies ($d_i = d$ when $N = 1$ in eq. 5). As it can be seen in the figure, relaxing the definition of LG galaxies through the distance measure d leads to an improvement on the frequency of LG-like galaxies (low d values). Evidently the distribution depends on the quantity used to define the galaxy, such a behaviour may help us to understand which are the most important quantities one may use to define the LG galaxies and may help us to understand the more complex results shown in figures 3 and 2.

Clearly from figure 4 we see that it is due to $M_{d,*}$ and $M_{b,*}$, the two quantities that more strongly deviate the population of galaxies from LG-like ones, having a mode tending to higher values of d and a very low amplitude tail to low d values. This might indicate that indeed are $M_{d,*}$ and $M_{b,*}$ the two numbers that must be most well constrained to be able to determine the probability distribution of LG-like galaxies. Curiously the quiet behaviour of the distribution of d values for the definition that uses $M_{d,gas}$ shows not to be too clustered, and clearly shows to be more common among the population of galaxies, while $V_{\rm cmax}$ still shows a peak close to $d \sim 0.7$ but even with that, it shows to have a frequency that is considerable at low d values. Note that $V_{\rm cmax}$ is a good tracer of the mass of the host halo, and that it is indeed the quantity that we use (implicitly) to constrain the galaxies by halo mass in the quite broad halo mass range we are working.

In general all distributions depends on the values of the parameters used to model the full galaxy population. In Figure 4 we show with each line a realisation of the galaxy set for a different value of $\alpha_{\rm out}$, as it was used in the figure 2. As it can be seen in that figure, the distribution of d changes for each run, however the differences between lines are not so big. The most noticeable differences are observed for $M_{b,*}$ and $V_{\rm cmax}$ where differently from what was observed in Figure 2 the fraction of objects with low d values increases for low values of $\alpha_{\rm out}$.

One may ask two questions: How is it possible to have, on the basis of the definition of d through only one parameter, a non-null fraction of LG-like galaxies, but absolutely no galaxy fulfilling the more robust (but stringent) definition using the four parameters simultaneously?. Why is the dependence on $\alpha_{\rm out}$ in figure 4 in contradiction with what was found in figure 2?

For the first question, a detailed analysis of the data shows that for a given value of the galactic property used to define d_i, it is in many cases anti-correlated with the others, so, for example, no many galaxies have low $\Delta M_{d,*}$. Galaxies with low $\Delta M_{b,*}$ have large $\Delta M_{d,*}$, intermediate-large $\Delta V_{\rm cmax}$ and galaxies with low $\Delta M_{d,g}$ have large $\Delta V_{\rm cmax}$, and $\Delta M_{d,*}$. All this together makes that under an individual quantity basis, it is possible to have a fraction of model galaxies with that quantity compatible with the definition of the LG-like galaxies. However when considering all the quantities simultaneously there is no way to fit all the observations that define our LG galaxies, since they exclude mutually.

The answer to the second question follows from the same argument. Although on the individual basis we may have trend for two of the quantities on variations of $\alpha_{\rm out}$, the complex way the combine, as exposed in the previous paragraph, is responsible for the behaviour seen in figure 2. Notice for example that in that figure, at high d again the distribution associated to low values of $\alpha_{\rm out}$ shows an increase, showing the remnant trend seen in figure 4 for individual quantities.

From this section we conclude three things:

1) It is difficult to reproduce simultaneously all properties of LG-like galaxies.

2) Defining them on the basis of only one quantity may increase the chance to reproduce the observations of the LG galaxies, however the combination of individual

[1] A similar plot for M31 can be found but since it looks very similar it is not necessary to show it.

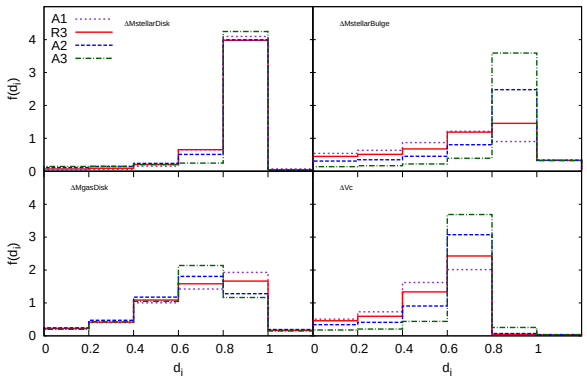

Figure 4. Distribution of d values relative the MW computed using only one of the quantities shown in each panel.

measurements noes not lead to a better chance of finding LG-like objects.

3) So defined, galaxies like the ones we find in the LG are difficult to reproduce and we could say they are improbable.

3.2 The LG candidates

Now we focus our attention on the candidates to MW and M31 galaxy in our constrained simulations and study how the properties of these galaxies change under variations of the model parameters. From the constrained simulations we took the merger trees of these two candidates to MW and M31 and ran our models several times variating smoothly the values of the parameters $\epsilon_\star$ and α_{out} and check how the galaxy properties change under such variations. In order to account for the variance on the results, for each galaxy defined by the couple of values ($\epsilon_\star$,α_{out}), we ran 100 realisations for each pair of values of the parameters. From that set we compute the median value of the galaxy properties that are presented in Figure 5.

In Figure 5 we show the different galaxy properties: gas-to-total mass fraction, stellar-to-total mass fraction and bulge-to-total mass fraction all as a function of the values of the parameters $\epsilon_\star$ and α_{out}. In that figure each line of plots is associated to the different realisations (10909, 16953 or 2710), since we have three different realisations providing three pairs of candidates.

Not all points in the plane are shown. In that figure we only show the points that fall inside the region of tolerance of the observational constrains imposed in table 1. Analysing this figure would lead us to conclude which are the best values of the parameters ($\epsilon_\star$, α_{out}) one can use to reproduce consistently the properties of the LG galaxies, or conversely, which are the values of the parameters that characterise the properties of the LG galaxies.

Ideally, the set of parameters ($\epsilon_\star$, α_{out}) that better describe the observations of the LG galaxies given the constraints on the three candidates would be that resulting from the intersection of the different data sets for the different properties. That is, the values of the parameters ($\epsilon_\star$, α_{out}) that are able to reproduce simultaneously the three observables for each candidate. These regions are shown in figure 5 for the MW galaxy. In that figure we can clearly see that depending on the realisation of the candidate there are different regions in the ($\epsilon_\star$, α_{out}) plane that satisfy the observational constraint. We can also see that for a given candidate the different properties can be reproduced differently by different values of the parameters. Is in this way that for example for the candidate 10909 almost all the plane in ($\epsilon_\star$, α_{out}) produces results that are consistent with the observations of M_*/M_{tot}, while almost none of these points in the same region of the plane produce results consistent with the observations of M_{bulge}/M_{tot} and only a reduced region of these parameters is allowed by the constrain of the observations of M_{gas}/M_{tot}. A similar behaviour can be seen for the candidates in the other two boxes.

Analysing in detail, for a given candidate, only a very small portion of the plane corresponding to the regions enclosed by the lines, are those that correspond to regions where there is agreement for the values of the parameters that reproduce the three observed constraints of the MW galaxy. No much agreement (in a point by point basis) between the different candidates is found. However, what can be seen is a clear trend on the values that favour the observations among the three candidates. Specifically, almost all values of $\epsilon_\star$ show to be able to reproduce the observed mass fractions. On the other hand, not all values of α_{out} seem to fit the constraint. Notice that values of α_{out} between 2.5 and 2.85 seems to favour the observables for all three candidates, in agreement with the results shown in section 3.1.

The scenario is quite more different for M31. As in can be seen in Figure 5 (bottom), there is no intersection between the regions on the plane ($\epsilon_\star$, α_{out}) that for a given candidate fits the observational constraints. Also, although in agreement with what is found for MW almost all values of $\epsilon_\star$ can satisfy the constraint, it is not as clear that large values of α_{out} do so, not at least with the clarity is can be seen for MW. Note also that in particular, M_*/M_{tot} is not well reproduced, in contrast to what is observed for MW and that in general the fraction of area in the plane M_*/M_{tot} is not well reproduced, in contrast to what is observed for the MW. Finally one can see that the fraction of area in the plane ($\epsilon_\star$, α_{out}) that is well described by the models is smaller. This may imply two possibilities: One, that the parameter describing both galaxies are very much different, or second, that as it was mentioned in the previous section, it is very difficult to fit simultaneously the observable properties of the galaxies in the local group, and it may be even more evident for M31.

4 SUMMARY AND DISCUSSION

We have used numerical simulations of galaxy formation to estimate the fraction of LG-like galaxies through the definition of a distance measure in a N-dimensional parameter space in a sample of around 27000 model galaxies. The outcome of this initiative can be summarised as:

1) Through the more stringent distance measure defined in eq. 5 the fraction of galaxies similar to MW and M31 is

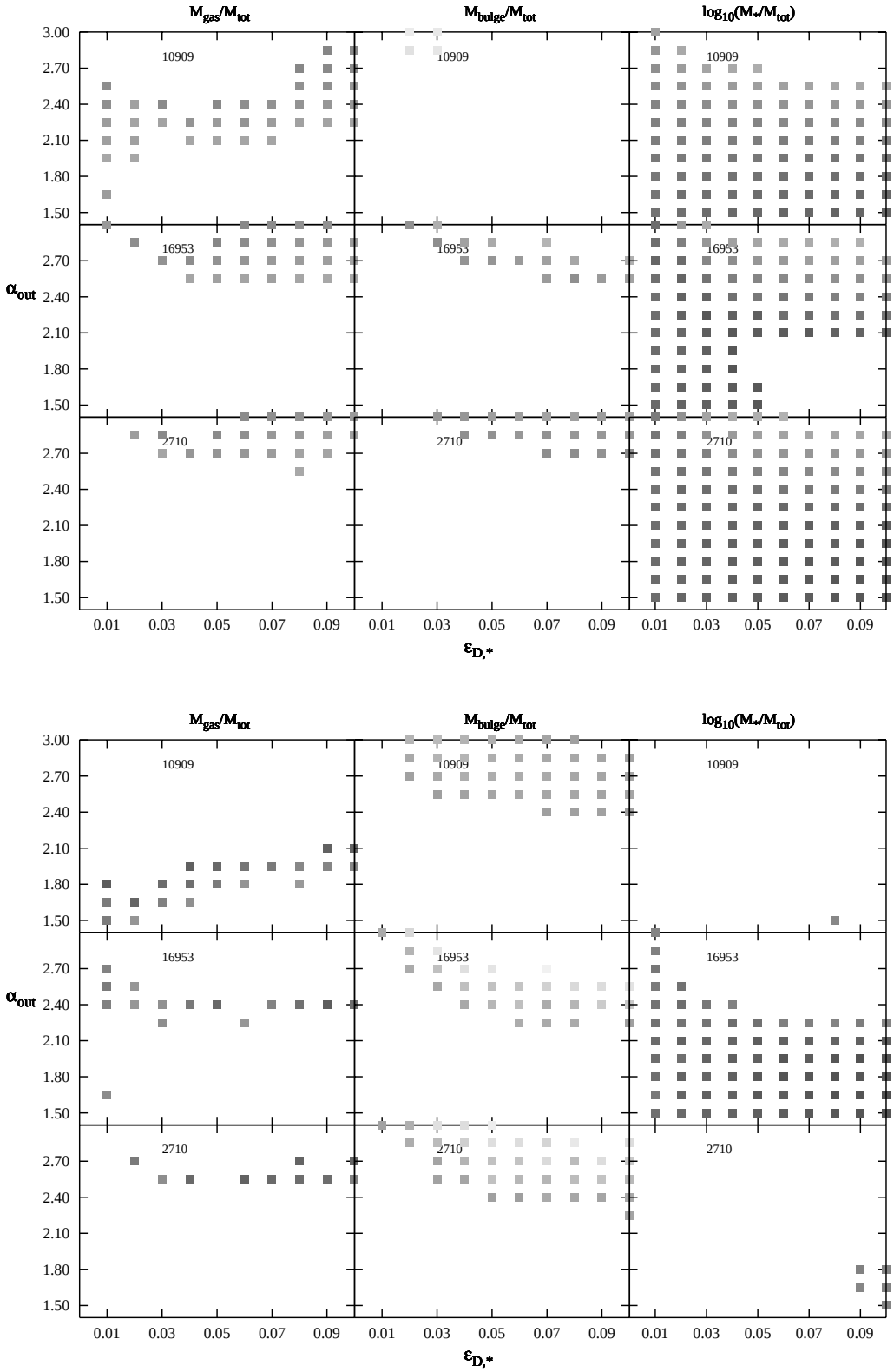

Figure 5. Mean gas mass fraction, Bulge mass and total stellar mass of realisations of the MW and M31 as a function of the values of the parameters $\epsilon_\star$ and $\alpha_{outflow}$. Only points falling in the ranges of values associated with the property of each galaxy are shown. Squares show the data for MW while triangles show the data for M31 while the grey scale indicates the different values of the property.

zero when one tries to fit simultaneously all observables used to define the LG galaxies.

2) Relaxing the form of the distance measure, and computing the distance in a parameter-by-parameter basis one can find that there are objects that fulfil the individual observational constraints, but that these objects that satisfy one or two parameters do not satisfy the others.

We have found however that in general all values of the parameter $\epsilon_\star$ may be in agreement with observational constraints, while larger values of α_{out} favour an increase in the frequency of LG-like objects.

The simulations used in this work are constrained simulations of the local Universe, and they have been ran in a way that a portion of the simulation volume should reproduce the large scale environment of the local group, as well as the small scale conditions to include a candidate to host a Local Group. Using this constraint we have ran several realisations of MW and M31 variating the model parameters ($\epsilon_\star$ and α_{out}) in order to find the region of this reduced parameter space that best reproduces the observations. In agreement with the findings of the first part of the paper, we found that the probability of reproducing simultaneously several properties of the LG galaxies is very low. Again we found that almost all values of $\epsilon_\star$ are in agreement with the observational constraints, while for MW values of α_{out} between 2.5 and 2.85 produce results that are in kind of agreement with the observations. For M31 the volume of parameter space sampled by the models is smaller, indicating that reproducing its properties is somehow more difficult than for MW, or that the range of physical parameters explaining the properties of both galaxies does not overlap evenly.

Considering the size of the sample, and the nature of the constraints (in the observations and in the simulations), a major conclusion out of this work is that the major galaxies in the Local Group are not that common.

In table **??** we have shown a larger plan of simulations that it was discussed in the results. Variations on the mass ratio η defining the nature of the mergers does not change the distributions of distance measures, that is, the galaxy population does not change (relative to LG galaxies) under variations of the mass threshold that defines the nature of the mergers, and therefore does not affect the fraction of LG-like galaxies in our simulations. Moving the material resulting from a merger to the bulge instead of the disk also show not to influence noticeably the final population of galaxies. It seems to be related to the quiet mass accretion history of the LG galaxies. As it has been shown in Forero-Romero et al. 2011, the MAH of LG haloes is quiet. They also show that in general its MAH does not bias from the general population of haloes in the same mass range. That the galaxy population nor the fraction of LG-like galaxies does not change much under variation of these parameters, is just a consequence of the uniformity on the distribution of MAH's in our simulations.

Note that in the first part of this work we do not constrain explicitly the mass of the dark matter haloes. The mass range we are using to study the fraction of LG-like galaxies is broad, 10^{11} to $10^{13}h^{-1}\,\mathrm{M}_\odot$, way much broader than any dark matter halo mass estimated for the galaxies in the Local Group. We use such a broad mass range just to allow a comparison with a larger halo and therefore galaxy population and to avoid the imposition of a biasing by the range of dark matter halo masses. However, the constraint in the halo mass comes in the distance measure through the maximum circular velocity of the galaxy V_{cmax}, which depends directly on the dark matter halo mass, but that is related to the observables, conversely to mass.

Implications:

de Rossi etal? Boylan-Kolchin?

ACKNOWLEDGEMENTS

The authors wants to tanks to DAAD and Colciencias for the financial support through the bilateral collaboration PPP-PROCOL. Project XXXXXXXX. J.C.M., J.F. and S.G. acknowledge the hospitality from Universidad de Antioquia. S.S. and J.Z. acknowledge the hospitality of the Leibniz Institut Für Astrophysik Potsdam.

REFERENCES

This paper has been typeset from a TEX/ LATEX file prepared by the author.